Advances in Physics Theories and Applications
ISSN 2224-719X (Paper) ISSN 2225-0638 (Online)
Vol.32, 2014

Magnetohydrodynamic Peristaltic flow of a couple stress with heat and mass transfer of a Jeffery fluid in a tube through porous medium

Dheia G. Salih Al-Hhafajy [1] and Ahmed Abdulhadi [2]

[1] Department of Math., College of Computer Science and Mathematics, University of Al-Qadissiya, Diwaniya-Iraq. E. mail: dr.dheia.g.salih@gmail.com

[2] Department of Mathematics, College of Science, University of Baghdad, Baghdad-Iraq.

Abstract

The effects couple stress on the unsteady flow of a couple stress fluid an incompressible non-Newtonian (Jeffrey) fluid through porous medium have been discussed. The thermal diffusion thermo effect are taken to our consideration. Analytical expression for the axial velocity, stream function and axial pressure gradient are established. The flow is investigated in a wave frame of reference moving with the velocity of the wave. The non-linear partial differential equations which govern this problem are simplified by making the assumptions of long wave length approximation. The analytical formula of the velocity and temperature have been obtained in terms of Bessel function of first and second kinds. In addition, it has been illustrated graphically for significant various parameters such as, magnetic parameter, couple stress parameter, permeability parameter, and thermal parameters .

Keywords : Magnetohydrodynamic, Peristaltic, couple stress fluid, Heat transfer, Porous medium**.**

1. Introduction

The study of peristaltic motion has gained considerable interest because of its extensive applications in urine transport from the kidney to bladder vasomotion of the small blood of the chyme in gastrointestinal tract, and so forth. Peristaltic pumping is found in many applications, for example, vessels movements, such as the transport of slurries, sensitive or corrosive fluids, sanitary fluid, and noxious fluids in the nuclear industry. The couple stress fluid is a special case of non-Newtonian fluid which is intended to take into account the particle size effects. The micro-continuum theory of couple stress fluid proposed by Stokes [6], defines the rotational field in terms of the velocity field for setting up the constitutive relationship between the stress and the strain rate . The couple stress model plays an important role in understanding some of the non-Newtonian flow properties of blood. A number of studies for couple stress and non-Newtonian fluids have been reported [1-7].

Theory of non-Newtonian fluids has received a great attention during the recent years, because the traditional viscous fluids cannot precisely describe the characteristics of many physiological fluids, see. Hayat & Ali [8]. Hayat et al. [9] have investigated the effects of compliant walls and porous space on the MHD peristaltic flow of Jeffery fluids. Srinivas [10] investigated the influence of heat and mass transfer on MHD peristaltic flow through a porous space with compliant walls. The influence of heat transfer and temperature dependent viscosity on peristaltic flow of a Jeffrey-six constant fluid has been studied by Nadeem [11]. Kothandapani [12] have analysed the MHD peristaltic flow of a viscous fluid in asymmetric channel with heat transfer. Kothandapani [13] studied the influence of wall properties in the MHD peristaltic transport with heat transfer and porous medium. Hayat & Ali [14] studied the peristaltic motion of a Jeffrey fluid in a tube with sinusoidal wave travelling down its wall.

Recently, the effect of magnetic field on viscous fluid has been reported for treatment of the following pathologies: Gastroenric pathologies, rheumatisms, constipation and hypertension that can be treated by placing one electrode either on the back or on the stomach and the other on the sole of the foot; this location will induce a better blood circulation. El-Dabe et al. [15] and [16] have been studied heat and mass transfer of a steady slow motion of a Rivilin-Ericksen fluid in tube of varying cross-section with suction. Also, they investigated the effect

of both magnetic field and porous medium on non-Newtonian fluid by studying the unsteady flow of a compressible biviscosity fluid in a circular tube, in which the flow is induced by a wave traveling on the tube wall. The incompressible flow of electrically conducting biviscosity fluid, through an axisymmetric non-uniform tube with a sinusoidal wave under the considerations of long wave length and law Reynolds number, is discussed by El-Dabe et al. [17].

The objective of this paper is to study the influence of couple stress, uniform magnetic field and permeability of the medium on the dynamics of unsteady flow of an incompressible Jeffrey fluid in a tube with heat and mass transfer. The governing equations of Jeffrey fluid in the cylindrical coordinates have been modeled. The equations are simplified using long wavelength and low Reynolds number approximations. The governing equations of fluid flow are solved subject to the relevant the boundary conditions, analytically. The effects of various parameters such as: magnetic parameter M^2, permeability k Reynolds number R_e, Prandtl number P_r, Schmidt number S_c, Soret number S_r on these solutions are discussed and illustrated graphically.

2. Mathematical Formulation

Consider a peristaltic flow of an incompressible Jeffrey fluid in a coaxial uniform circular tube. The cylindrical coordinates are considered, where R is along the radius of the tube and Z coincides with the axes of the tube as shown in figure (1). A uniform magnetic field B_0 is imposed and acting along axis.

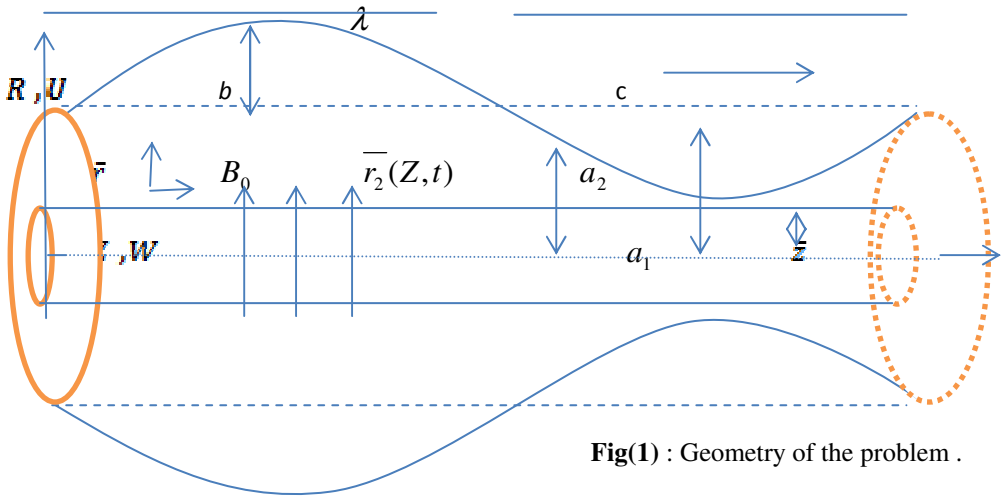

Fig(1) : Geometry of the problem .

The geometry of wall surface is described as:

$$H(\bar{Z},\bar{t}) = a + b.Sin[\frac{2\pi}{\lambda}(\bar{Z} - c\bar{t})] \qquad (1)$$

Where a is the average radius of the undisturbed tube, b is the amplitude of the peristaltic wave, λ is the wavelength, c is the wave propagation speed, and $\bar{t}$ is the time.

3. Basic equations

The basic equations governing the non-Newtonian Jeffrey fluid are given by:

The continuity equation is given by:

$$\nabla \bar{V} = 0 \qquad (2)$$

The momentum equation with couple-stress fluid are:

$$\rho(\bar{V}.\nabla)\bar{V} = \nabla\bar{\tau} + \mu_e.\bar{J}\times\bar{B} - \frac{\mu}{K^*}\bar{V} - \bar{\eta}.\nabla^4\bar{V} \tag{3}$$

The temperature equation is given by:

$$c_p.\rho(\bar{V}.\nabla)T = k.\nabla^2 T - \nabla.q_r - QT \tag{4}$$

where $\nabla^2 = \frac{1}{r}\frac{\partial}{\partial r}(r\frac{\partial}{\partial r})$ (Laplace operator) and $\nabla^4 = \nabla^2(\nabla^2)$. Also $\bar{V}$ is the velocity, μ is the dynamic viscosity, K^* is the permeability, $\bar{B} = (0, B_0, 0)$ is the magnetic field, σ is the electrical conductivity, μ_e is the magnetic permeability, $\bar{\tau}$ is the Cauchy stress tensor, and $\bar{\eta}$ is the constant associated with the couple stress. Too, T is the temperature of the fluid, k is the thermal conductivity and c_p is the specific heat capacity at constant pressure.

The constitutive equations for an incompressible Jeffrey fluid are given by:

$$\bar{\tau} = -\bar{P}\bar{I} + \bar{S} \quad , \quad \bar{S} = \frac{\mu}{1+\lambda_1}(\bar{\gamma} + \lambda_2\dot{\bar{\gamma}}) \tag{5}$$

where $\bar{S}$ is the extra stress tensor, $\bar{P}$ is the pressure, $\bar{I}$ is the identity tensor, λ_2 is the ratio of relaxation to retardation times, $\bar{\gamma}$ is the shear rate and λ_2 is the retardation time.

4. Method of solution

Let $\bar{U}$ and $\bar{W}$ be the velocity components in the radial and axial directions in the fixed frame respectively.

For the unsteady two-dimensional flow, the velocity components may be written as follows:

$$\bar{V} = (\bar{U}(\bar{r},\bar{z}), \bar{W}(\bar{r},\bar{z}), 0) \tag{6}$$

Also, the temperature function may be written as follows:

$$T = T(r,z). \tag{7}$$

The equations of motion (2)-(4) and the constitutive relations (5) take the form:

$$\frac{\partial\bar{U}}{\partial\bar{R}} + \frac{\bar{U}}{\bar{R}} + \frac{\partial\bar{W}}{\partial\bar{Z}} = 0, \tag{8}$$

$$\rho(\frac{\partial\bar{U}}{\partial\bar{t}} + \bar{U}\frac{\partial\bar{U}}{\partial\bar{R}} + \bar{W}\frac{\partial\bar{W}}{\partial\bar{Z}}) = -\frac{\partial\bar{p}}{\partial\bar{R}} + \frac{1}{\bar{R}}\frac{\partial}{\partial\bar{R}}(\bar{R}\bar{S}_{\bar{R}\bar{R}}) + \frac{\partial}{\partial\bar{Z}}(\bar{S}_{\bar{R}\bar{Z}}) - \frac{\bar{S}_{\bar{\theta}\bar{\theta}}}{\bar{R}} - \frac{\mu}{k}\bar{U} - \bar{\eta}.\nabla^4\bar{U}, \tag{9}$$

$$\rho(\frac{\partial\bar{U}}{\partial\bar{t}} + \bar{U}\frac{\partial\bar{U}}{\partial\bar{R}} + \bar{W}\frac{\partial\bar{W}}{\partial\bar{Z}}) = -\frac{\partial\bar{p}}{\partial\bar{Z}} + \frac{1}{\bar{R}}\frac{\partial}{\partial\bar{R}}(\bar{R}\bar{S}_{\bar{R}\bar{Z}}) + \frac{\partial}{\partial\bar{Z}}(\bar{S}_{\bar{Z}\bar{Z}}) - \frac{\mu}{k}\bar{W} - \sigma B_o^2\bar{W} - \bar{\eta}.\nabla^4\bar{W}, \tag{10}$$

$$\frac{\partial T}{\partial t}+\bar{U}\frac{\partial T}{\partial \bar{R}}+\bar{W}\frac{\partial T}{\partial \bar{Z}}=\frac{k}{c_p\rho}\left(\frac{\partial^2 T}{\partial \bar{R}^2}+\frac{1}{\bar{R}}\frac{\partial T}{\partial \bar{R}}+\frac{\partial^2 T}{\partial \bar{Z}^2}\right)-\frac{16\sigma_o T_2^E}{3k_o}\frac{1}{\bar{R}}\frac{\partial}{\partial \bar{R}}\left(\bar{R}\frac{\partial T}{\partial \bar{R}}\right)-QT,$$

(11)

In the fixed coordinates $(\bar{R},\bar{Z})$ the flow between the two tubes is unsteady. It becomes steady in a wave frame $(\bar{r},\bar{z})$ moving with the same speed as wave in the $\bar{Z}$-direction. The transformations between the two frames is given by:

$$\bar{r}=\bar{R},\ \bar{z}=\bar{Z}-c\bar{t} \tag{12}$$

$$\bar{u}=\bar{U},\bar{w}=\bar{W}-c \tag{13}$$

where $(\bar{r},\bar{z})$ and $(\bar{U},\bar{W})$ are the velocity components in the moving and fixed frames, respectively . After using these transformation, the equations of motion are;

$$\frac{\partial \bar{u}}{\partial \bar{r}}+\frac{\bar{u}}{\bar{r}}+\frac{\partial \bar{w}}{\partial \bar{z}}=0, \tag{14}$$

$$\rho\left(\bar{u}\frac{\partial \bar{u}}{\partial \bar{r}}+\bar{w}\frac{\partial \bar{w}}{\partial \bar{z}}\right)=-\frac{\partial \bar{p}}{\partial \bar{r}}+\frac{1}{\bar{r}}\frac{\partial}{\partial \bar{r}}(\bar{r}\bar{S}_{\bar{r}\bar{r}})+\frac{\partial}{\partial \bar{z}}(\bar{S}_{\bar{r}\bar{z}})-\frac{\bar{S}_{\bar{\theta}\bar{\theta}}}{\bar{r}}-\frac{\mu}{k}\bar{u}-\bar{\eta}.\nabla^4\bar{u}, \tag{15}$$

$$\rho\left(\bar{u}\frac{\partial \bar{u}}{\partial \bar{r}}+\bar{w}\frac{\partial \bar{w}}{\partial \bar{z}}\right)=-\frac{\partial \bar{p}}{\partial \bar{z}}+\frac{1}{\bar{r}}\frac{\partial}{\partial \bar{r}}(\bar{r}\bar{S}_{\bar{r}\bar{z}})+\frac{\partial}{\partial \bar{z}}(\bar{S}_{\bar{z}\bar{z}})-\frac{\mu}{k}\bar{w}-\sigma B_o^2(\bar{w}+c)-\bar{\eta}.\nabla^4\bar{w}, \tag{16}$$

$$\bar{u}\frac{\partial T}{\partial \bar{r}}+\bar{w}\frac{\partial T}{\partial \bar{z}}=\frac{k}{c_p\rho}\left(\frac{\partial^2 T}{\partial \bar{r}^2}+\frac{1}{\bar{r}}\frac{\partial T}{\partial \bar{r}}+\frac{\partial^2 T}{\partial \bar{z}^2}\right)+\frac{16\sigma_o T_2^E}{3k_o}\frac{1}{\bar{r}}\frac{\partial}{\partial \bar{r}}\left(\bar{r}\frac{\partial T}{\partial \bar{r}}\right)-QT, \tag{17}$$

where $\bar{u}$ and $\bar{w}$ are the velocity components in the $\bar{r}$ and $\bar{z}$ directions, respectively, ρ is the density, $\bar{p}$ is the pressure, μ is the viscosity.

The appropriate boundary conditions are:

$$\left.\begin{array}{ll}\bar{w}=-1,\bar{u}=0,T=T_1 & \text{at}\quad \bar{r}=\bar{r}_1=\varepsilon \\ \bar{w}=-1,\bar{u}=0,T=T_0 & \bar{r}=\bar{r}_2(\bar{z},\bar{t})=1+\phi.\sin(2\pi\bar{z})\end{array}\right\} \tag{18}$$

In order to simplify the governing equations of the motion, we may introduce the following dimensionless transformations as follows:

$$\left.\begin{array}{l} r=\frac{\bar{r}}{a_2},z=\frac{\bar{z}}{\lambda},\delta=\frac{a_2}{\lambda},u=\frac{\lambda\bar{u}}{a_2c},w=\frac{\bar{w}}{c},p=\frac{a_2^2\bar{p}}{\mu\lambda c},\bar{\alpha}=\alpha a_2=\sqrt{\frac{\mu}{\eta}}a_2, \\ S=\frac{a_2\bar{S}}{\mu c},r_1=\frac{\bar{r}_1}{a_2}=\varepsilon,r_2=\frac{\bar{r}_2}{a_2}=1+\phi.\sin(2\pi\bar{z}),\phi=\frac{b}{a_2},\vartheta=\frac{T-T_0}{T_1-T_0}\end{array}\right\} \tag{19}$$

where ϕ is the amplitude ratio, δ is the dimensionless wave number and $\bar{\alpha}$ is the couple stress fluid parameter indicating the ratio of the tube radius (constant) to material characteristic length ($\sqrt{\frac{\eta}{\mu}}$, has the dimension of length) .

Substituting (19) into equations (14)-(17), and simplify we obtain the following non-dimensional equations :

$$\left(\frac{\partial u}{\partial r}+\frac{u}{r}+\frac{\partial w}{\partial z}\right)=0, \tag{20}$$

$$R_e.\delta^3\left(u\frac{\partial u}{\partial r}+w\frac{\partial u}{\partial z}\right)=-\frac{\partial p}{\partial r}+\delta\frac{1}{r}\frac{\partial}{\partial r}(rS_{rr})+\delta^2\frac{\partial}{\partial z}(S_{rz})-\frac{\delta}{r}S_{\theta\theta}-\frac{a_2}{k}\delta^2u-\frac{\delta^2}{\alpha^2}.\nabla^4u, \tag{21}$$

$$R_e.\delta\left(u\frac{\partial w}{\partial r}+w\frac{\partial w}{\partial z}\right)=-\frac{\partial p}{\partial z}+\frac{S_{rz}}{r}+\frac{\partial S_{rz}}{\partial z}+\delta\frac{\partial S_{zz}}{\partial z}-(M^2+\frac{1}{D_a})w-M^2-\frac{1}{\alpha^2}.\nabla^4w, \tag{22}$$

$$\delta\left(u\frac{\partial\theta}{\partial r}+w\frac{\partial\theta}{\partial z}\right)=\frac{1}{P_r}\left(\frac{\partial^2\theta}{\partial r^2}+\frac{1}{r}\frac{\partial\theta}{\partial r}+\delta^2\frac{\partial^2\theta}{\partial z^2}\right)+\frac{4}{3R_n}\frac{1}{r}\frac{\partial}{\partial r}(r\frac{\partial\theta}{\partial r})-\Omega\theta, \tag{23}$$

where

$$S_{rr}=\frac{2\delta}{1+\lambda_1}\left[1+\frac{c\lambda_2\delta}{a_2}\left(u\frac{\partial}{\partial r}+w\frac{\partial}{\partial z}\right)\right]\left(\frac{\partial u}{\partial r}\right), \tag{24}$$

$$S_{rz}=\frac{1}{1+\lambda_1}\left[1+\frac{c\lambda_2\delta}{a_2}\left(u\frac{\partial}{\partial r}+w\frac{\partial}{\partial z}\right)\right]\left(\frac{\partial w}{\partial r}+\delta^2\frac{\partial u}{\partial z}\right), \tag{25}$$

$$S_{\theta\theta}=\frac{2\delta}{1+\lambda_1}\left[1+\frac{c\lambda_2\delta}{a_2}\left(u\frac{\partial}{\partial r}+w\frac{\partial}{\partial z}\right)\right]\left(\frac{u}{r}\right), \tag{26}$$

$$S_{zz}=\frac{2\delta}{1+\lambda_1}\left[1+\frac{c\lambda_2\delta}{a_2}\left(u\frac{\partial}{\partial r}+w\frac{\partial}{\partial z}\right)\right]\left(\frac{\partial w}{\partial z}\right). \tag{27}$$

Where, the previous dimensionless parameters (R_e the Reynolds number, P_r the Prandtl number, R_n the Radiation parameter, D_a the Darcy number and M^2 the magnetic parameter) are defined by:

$$R_e=\frac{c\rho a_2}{\mu},\ P_r=\frac{\mu c_p}{k},\ R_n=\frac{\rho k_0 c_p\nu}{4T_2^2\sigma_0},\ D_a=\frac{k}{a_2^2},\ M^2=\frac{\sigma B_0^2a_2^2}{\mu}$$

The related boundary conditions in the wave frame are given by:

$$\left.\begin{array}{l}w=-1,u=0,\vartheta=1\\ w=-1,u=0,\vartheta=0\end{array}\right\}\ \text{at}\ \left.\begin{array}{c}r=r_1=\varepsilon\\ r=r_2=1+\phi.\sin(2\pi z)\end{array}\right\} \tag{28}$$

The general solution of the governing equations (20)-(23) in the general case seems to be impossible; therefore, we shall confine the analysis under the assumption of small dimensionless wave number. It follows that $\delta \ll 1$. In other words, we considered the long-wavelength approximation. Along to this assumption, equations (20)-(23) become:

$$\frac{\partial u}{\partial r}+\frac{u}{r}+\frac{\partial w}{\partial z}=0, \tag{29}$$

$$\frac{\partial p}{\partial r}=0, \tag{30}$$

$$\frac{\partial p}{\partial z}+M^2=\frac{1}{r(1+\lambda_1)}\frac{\partial w}{\partial r}+\frac{\partial}{\partial r}\left(\frac{1}{(1+\lambda_1)}\frac{\partial w}{\partial r}\right)-(M^2+\frac{1}{D_a})w-\frac{1}{\alpha^2}.\nabla^4 w, \tag{31}$$

$$\left(\frac{1}{R_e P_r}+\frac{4}{3R_n}\right)\left(\frac{\partial^2\theta}{\partial r^2}+\frac{1}{r}\frac{\partial\theta}{\partial r}\right)-\Omega\theta=0, \tag{32}$$

Assuming the components of the couple stress tensor at the wall to be zero [7], we have the following dimensionless boundary conditions:

$$\left.\begin{aligned} w=-1,\ \frac{\partial^2 w}{\partial r^2}-\frac{\eta'}{r}\frac{\partial w}{\partial r}=0 \quad & r=r_1=\varepsilon \\ w=-1,\ \frac{\partial^2 w}{\partial r^2}-\frac{\eta'}{r}\frac{\partial w}{\partial r}=0 \quad & r=r_2 \end{aligned}\right\} \text{ at} \tag{33}$$

where $\eta'=\bar{\eta}/\eta$ is a couple stress fluid parameter ($\bar{\eta}$ and η are constants associated with the couple stress, when $\eta'\to 1$ (i.e. $\bar{\eta}'\to\eta$) no couple stress effect; Newtonian fluid [6-8]) .

5. Solution of the problem

Equation (30) shows that p dependents on z only. The general solution of Eq. (31) is

$$w=B_1 I_0(\lambda r\sqrt{|s_1|})+B_2 K_0(\lambda r\sqrt{|s_1|})+B_3 I_0(\lambda r\sqrt{|s_2|})+B_4 K_0(\lambda r\sqrt{|s_2|})-\frac{M^2+\frac{dp}{dz}}{M^2+\frac{1}{D_a}} \tag{34}$$

Where $s_1=-\frac{b_1}{\lambda^2}-\sqrt{\left(\frac{b_1}{\lambda^2}\right)^2-1}$, $s_2=-\frac{b_1}{\lambda^2}+\sqrt{\left(\frac{b_1}{\lambda^2}\right)^2-1}$, $b_1=\frac{\alpha^2}{2(1+\lambda_1)}$, and $\lambda^4=\alpha^2\left(M^2+\frac{1}{D_a}\right)$, also I_0 and K_0 are the modified Bessel functions of the first and second kind of order zero. B_1 , B_2 , B_3 and B_4 are constants can be determinates by using the boundary conditions Eq. (28) and Eq. (33) and will not mentioned here for the sake of simplicity.

The corresponding stream function ($u = -\frac{1}{r}\frac{\partial \psi}{\partial z}$ and $w = \frac{1}{r}\frac{\partial \psi}{\partial z}$) is

$$\psi = \frac{r^2}{2}\left(-\frac{M^2 + \frac{dp}{dz}}{M^2 + \frac{1}{D_a}}\right) - \frac{B_2 r K_1(ru_1)}{u_1} - \frac{B_4 r K_1(ru_2)}{u_2} + \frac{1}{2}B_1 r^2\,{}_0F_1\left(2, \frac{r^2u_1^2}{4}\right) + \frac{1}{2}B_{31} r^2\,{}_0F_1\left(2, \frac{r^2u_2^2}{4}\right) \tag{35}$$

Where $u_1 = \lambda\sqrt{|s_1|}$, $u_2 = \lambda\sqrt{|s_2|}$, and K_1, ${}_0F_1$ are the modified Bessel function of the second kind and Hypergeometric regularized function, respectively.

The instantaneous volume flow rate $Q(z)$ $(= 2\int_{r_1}^{r_2} rw\,dr)$ is given by;

$$\frac{dp}{dz} = M^2 - \left(\frac{M^2 + \frac{1}{D_a}}{(r_2^2 - r_1^2)}\right)\left\{\begin{array}{l} Q(z) + \frac{2B_2}{u_1}\left[r_2K_1(r_2u_1) - r_1K_1(r_1u_1)\right] + \frac{2B_4}{u_2}\left[r_2K_1(r_2u_2) - r_1K_1(r_1u_2)\right] - B_1\left\{r_2^2\,{}_0F_1\left(2, \frac{r_2^2u_1^2}{4}\right) - r_1^2\,{}_0F_1\left(2, \frac{r_2^2u_1^2}{4}\right)\right\} \\ - B_3\left\{r_2^2\,{}_0F_1\left(2, \frac{r_2^2u_2^2}{4}\right) - r_1^2\,{}_0F_1\left(2, \frac{r_2^2u_2^2}{4}\right)\right\} \end{array}\right\} \tag{36}$$

Following the analysis given by Shapiro et al. [18], the mean volume flow, q over a period is obtained as

$$q = Q + \frac{1}{2}(1 - \varepsilon^2 + \frac{\phi^2}{2}) \tag{37}$$

Which on using Eq. (36) yields

$$\frac{dp}{dz} = M^2 - \left(\frac{M^2 + \frac{1}{D_a}}{(r_2^2 - r_1^2)}\right)\left\{\begin{array}{l} q - \frac{1}{2}(1 - \varepsilon^2 + \frac{\phi^2}{2}) + \frac{2B_2}{u_1}\left[r_2K_1(r_2u_1) - r_1K_1(r_1u_1)\right] + \frac{2B_4}{u_2}\left[r_2K_1(r_2u_2) - r_1K_1(r_1u_2)\right] \\ - B_1\left\{r_2^2\,{}_0F_1\left(2, \frac{r_2^2u_1^2}{4}\right) - r_1^2\,{}_0F_1\left(2, \frac{r_2^2u_1^2}{4}\right)\right\} - B_3\left\{r_2^2\,{}_0F_1\left(2, \frac{r_2^2u_2^2}{4}\right) - r_1^2\,{}_0F_1\left(2, \frac{r_2^2u_2^2}{4}\right)\right\} \end{array}\right\} \tag{38}$$

The pressure rise Δp and the friction force (at the wall) on the outer and inner tubes are $F^{(o)}$ and $F^{(i)}$, respectively, in a tube of length ***L***, in their non-dimensional forms, are given by:

$$\Delta p = \int_0^1 \left(\frac{dp}{dz}\right) dz\,, \tag{39}$$

$$F^{(0)} = \int_0^1 r_2^2 \left(-\frac{dp}{dz}\right) dz\,, \tag{40}$$

$$F^{(i)} = \int_0^1 r_1^2 \left(-\frac{dp}{dz}\right) dz\,, \tag{41}$$

Substituting Eq. (58) in to Eqs. (39)-(41) with $r_1 = \varepsilon$, $r_2 = 1 + \phi\sin(2\pi z)$, we obtain the pressure rise and the friction force (at the wall of the outer and inner surfaces) .

The heat equation solution is found to be;

$$\theta = B_5 I_0(r\sqrt{A}) + B_6 K_0(r\sqrt{A}) \tag{42}$$

where $A = \dfrac{\Omega}{\left(\dfrac{1}{R_e P_r} + \dfrac{4}{3R_n}\right)}$. And by using the boundary conditions Eq. (28), we have

$$B_5 = \frac{K_0(r_2\sqrt{A})}{I_0(r_1\sqrt{A})K_0(r_2\sqrt{A}) - I_0(r_2\sqrt{A})K_0(r_1\sqrt{A})} \quad \text{and} \quad B_6 = -\frac{I_0(r_2\sqrt{A})B_5}{K_0(r_2\sqrt{A})} .$$

6. Numerical Results and Discussion

In this section, the numerical and computational results are discussed for the problem of an incompressible non-Newtonian Jeffrey fluid in a tube with heat and mass transfer through the graphical illustrations. The salient feature of peristaltic flow of couple-stress fluids through the porous medium are discussed through Figures (2-19). MATHEMATICA program is used to find out numerical results and illustrations.

Based on Eq. 39, Figs.(2-4) illustrates the effects of the parameters ε, α and M on the pressure rise Δp versus η, ϕ, and q, respectively. Fig.2 shows that the variation of Δp vs. η. We see that Δp increases with the increases of any one of α or M. While Δp decreases with the increases of ε.

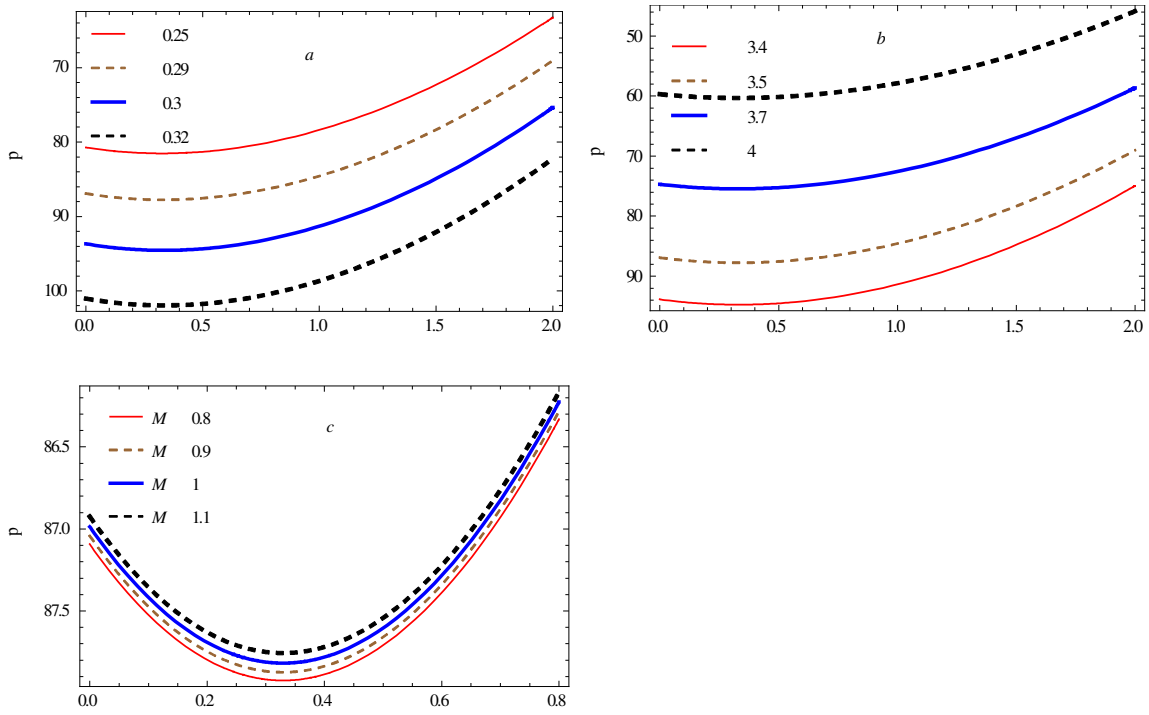

Fig.2 Plot showing variation of pressure rise Δp vs. η, at $D_a = 0.9, \lambda_1 = 0.1, q = 0.5, \phi = 0.1$ for (a) different values of ε, at $M = 1.1, \alpha = 3.5$, (b) different values of couple-stress parameter α, at $M = 1.1, \varepsilon = 0.3$, and (c) different values of magnetic parameter M, at $\alpha = 3.5, \varepsilon = 0.3$.

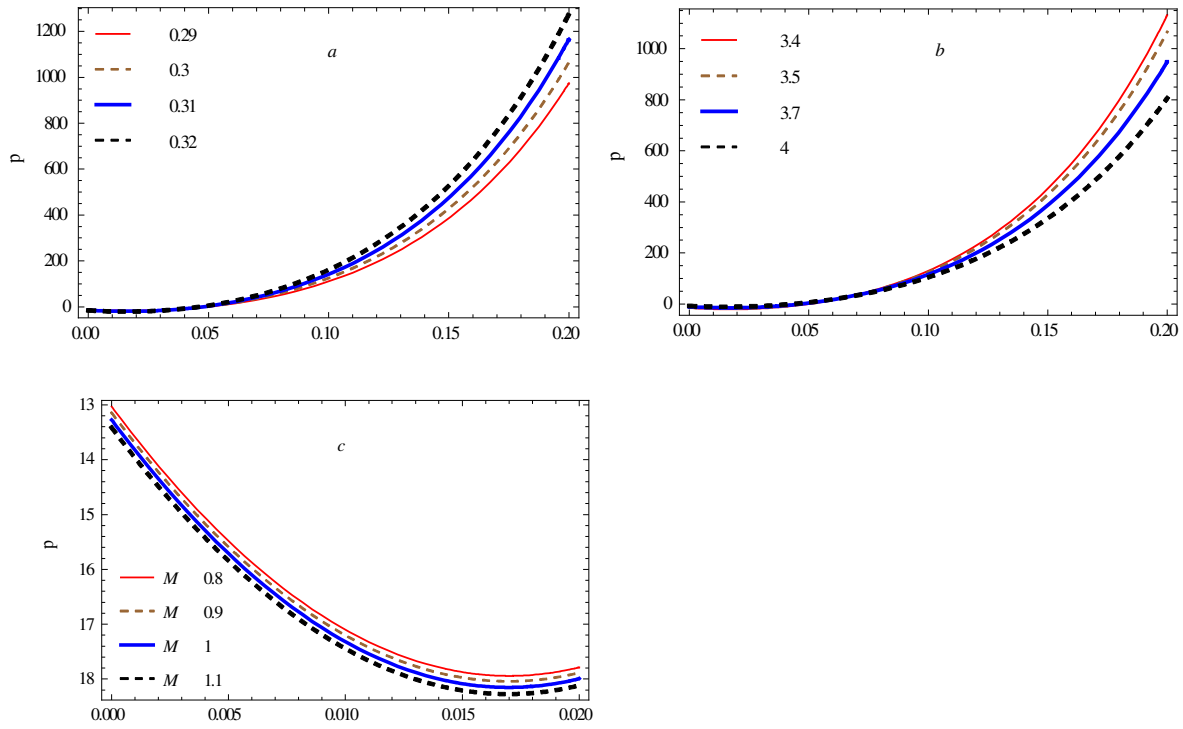

Fig.3 Plot showing variation of pressure rise Δp vs. ϕ, at $D_a=0.9, \lambda_1=0.1, q=0.5, \eta=0.5$ for (a) different values of ε, at $M=1.1, \alpha=3.5$, (b) different values of couple-stress parameter α, at $M=1.1, \varepsilon=0.3$, and (c) different values of magnetic parameter M, at $\alpha=3.5, \varepsilon=0.3$.

Fig.3 shows that the variation of Δp vs. ϕ. We see that Δp increases with the increasing of ε. And Δp decreases with the increasing of any one of α or M.

Fig.4 shows that the variation of Δp vs. q. In (a) we see that Δp increases with the increasing of ε in $0 < q < 0.62$, and Δp decreases with the increasing of ε when $0.62 < q$. From (b) it is found that Δp decreases with the increasing of α in $q < 0.719$, and Δp increases with the increasing of α when $q > 0.719$.And (c) show that Δp decreases with the increasing of M.

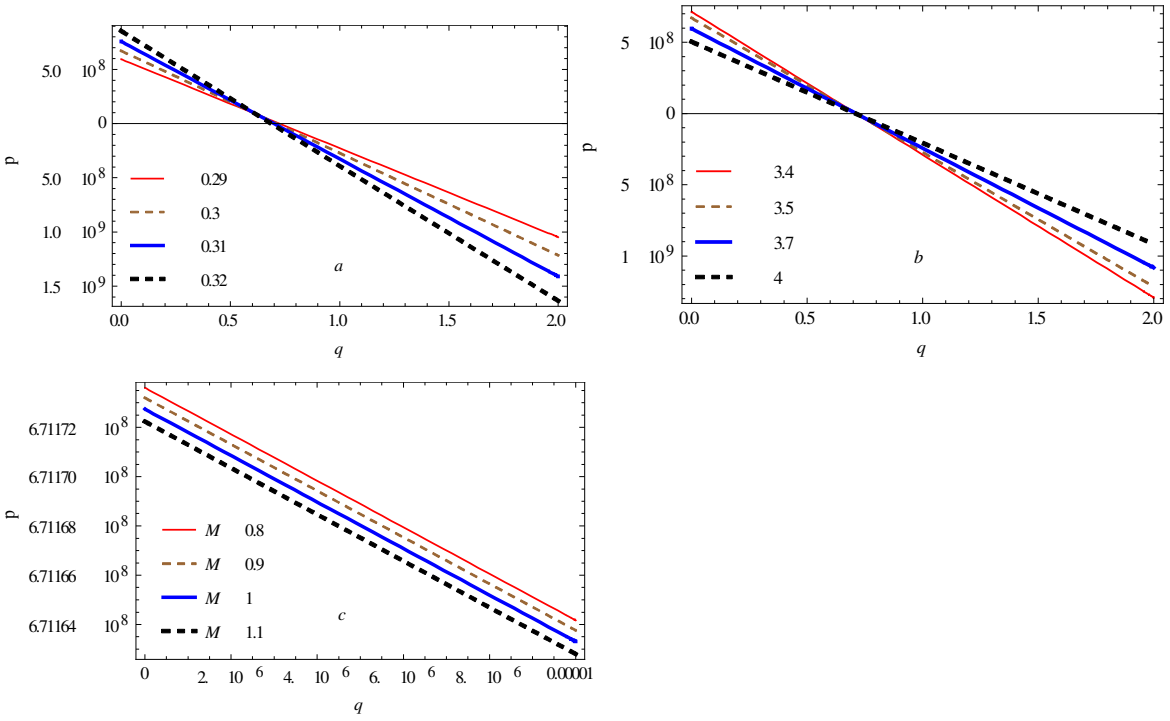

Fig.4 Plot showing variation of pressure rise Δp vs. q , at D_a =0.9, λ_1 =0.1, ϕ=0.5, η=0.5 for (a) different values of ε , at M = 1.1, α = 3.5 , (b) different values of couple-stress parameter α , at M = 1.1, ε = 0.3 , and (c) different values of magnetic parameter M , at α = 3.5, ε = 0.3 .

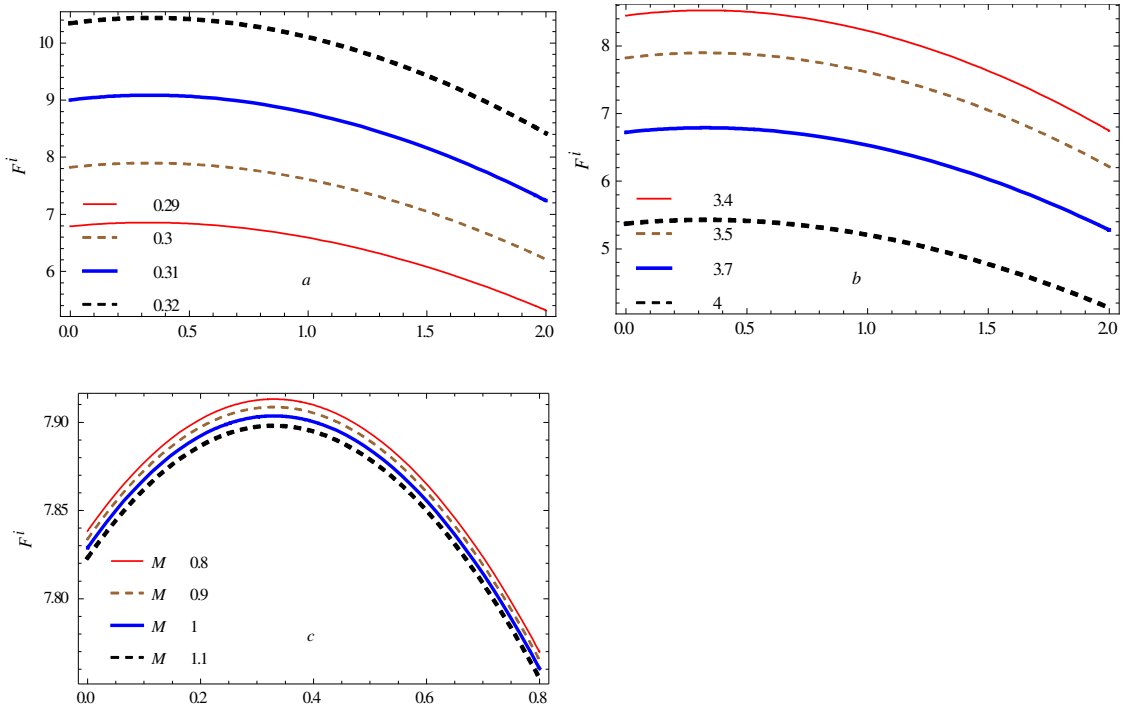

Fig.5 Plot showing variation of $F^{(i)}$ vs. η, at $D_a=0.9, \lambda_1=0.1, \phi=0.1, q=0.5$, for (a) different values of ε, at $M=1.1, \alpha=3.5$, (b) different values of couple-stress parameter α, at $M=1.1, \varepsilon=0.3$, and (c) different values of magnetic parameter M, at $\alpha=3.5, \varepsilon=0.3$.

Based on Eq. 40, Figs.(5-7) illustrates the effects of the parameters ε, α and M on the inner friction force $F^{(i)}$ versus η, ϕ, and q, respectively. Fig.5 shows that the variation of $F^{(i)}$ vs. η. We see that $F^{(i)}$ increases with the increasing of ε. While $F^{(i)}$ decreases with the increasing of any one of α or M. Fig.6 shows that the variation of $F^{(i)}$ vs. ϕ. $F^{(i)}$ decreases with the increasing of ε. And $F^{(i)}$ increases with the increasing of any one of α or M.

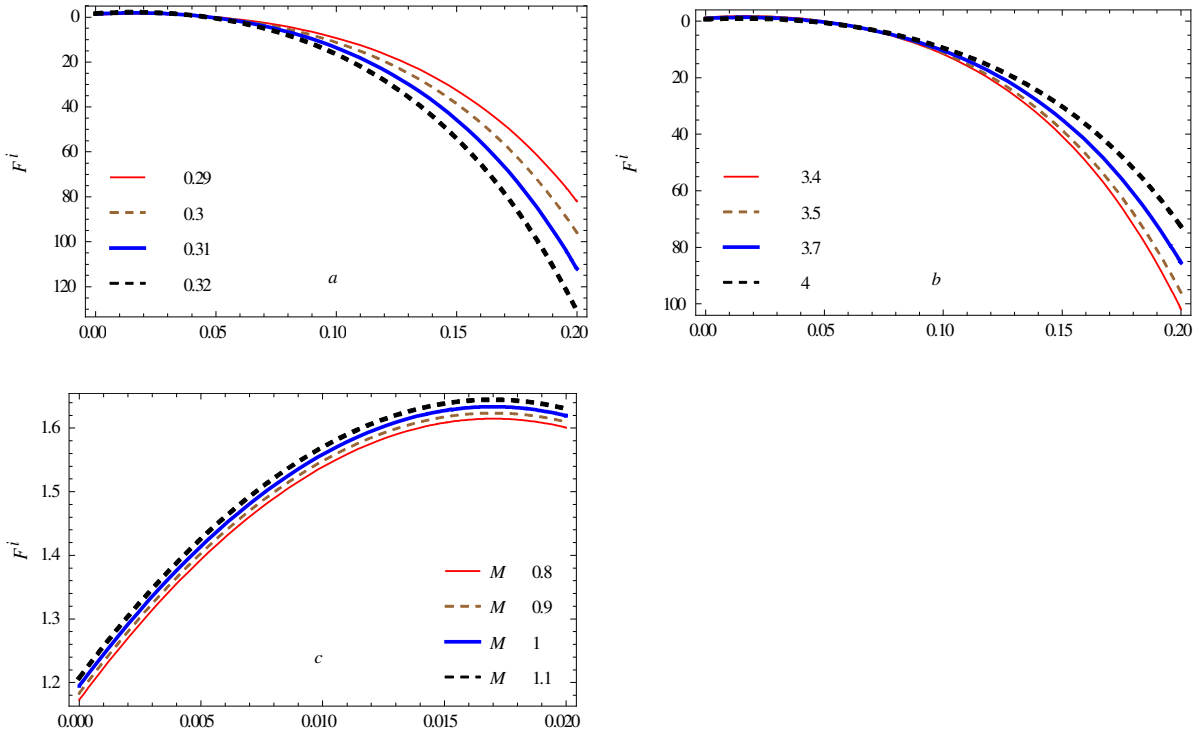

Fig.6 showing variation of $F^{(i)}$ vs. ϕ, at D_a=0.9,λ_1=0.1,η=0.5,q=0.5, for (a) different values of ε, at $M = 1.1, \alpha = 3.5$, (b) different values of couple-stress parameter α, at $M = 1.1, \varepsilon = 0.3$, and (c) different values of magnetic parameter M, at $\alpha = 3.5, \varepsilon = 0.3$.

Fig.7 shows that the variation of $F^{(i)}$ vs. q. In (a) we see that $F^{(i)}$ decreases with the increasing of ε when $q <$ 0.65, and $F^{(i)}$ increases with the increasing of ε when $q >$ 0.65. From (b) it is found that $F^{(i)}$ increases with the increasing of α when $q <$ 0.72, and $F^{(i)}$ decreases with the increasing of α when $q >$ 0.72. And (c) show that $F^{(i)}$ increases with the increasing of M.

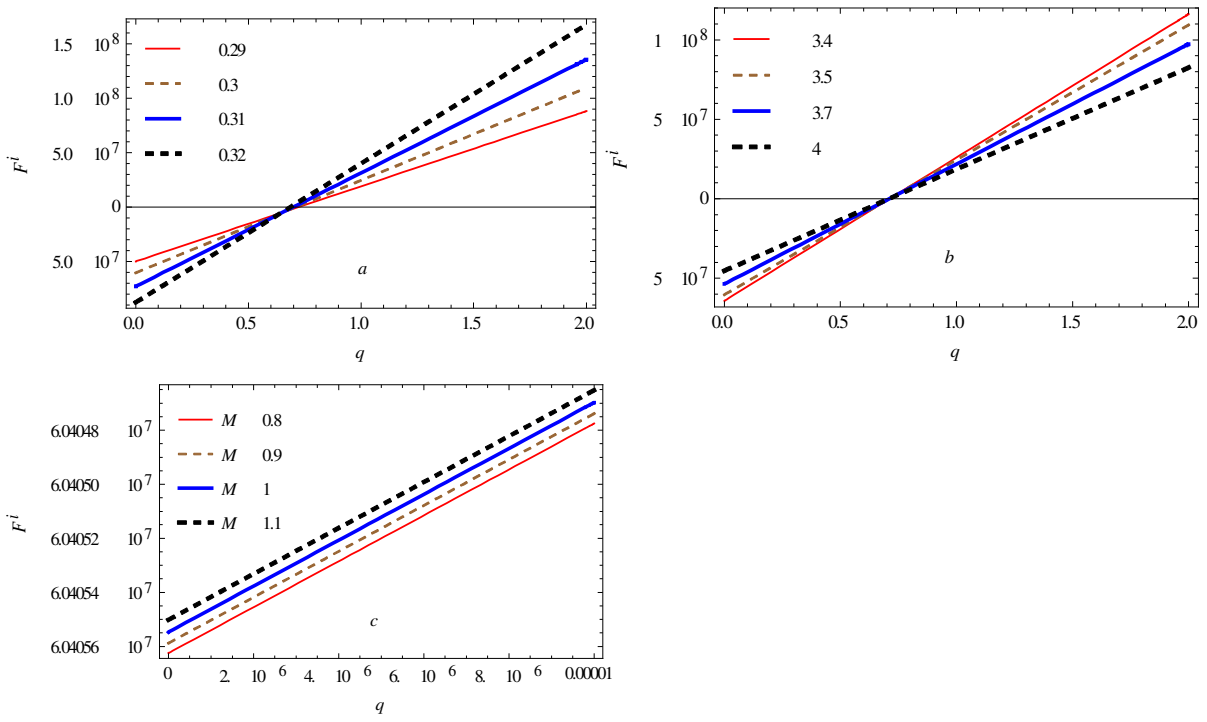

Fig.7 showing variation of $F^{(i)}$ vs. q, at D_a=0.9,λ_1=0.1,η=0.5,ϕ=0.5, for (a) different values of ε, at $M=1.1,\alpha=3.5$, (b) different values of couple-stress parameter α, at $M=1.1,\varepsilon=0.3$, and (c) different values of magnetic parameter M, at $\alpha=3.5,\varepsilon=0.3$.

Based on Eq. 41, Figs.(8-10) illustrates the effects of the parameters ε, α, and M on the outer friction force $F^{(o)}$ versus η, ϕ, and q, respectively. Fig.8 shows that the variation of $F^{(o)}$ vs. η. We see that $F^{(o)}$ increases with the increasing of ε, while $F^{(o)}$ decreases with the increasing of any one of α or M.

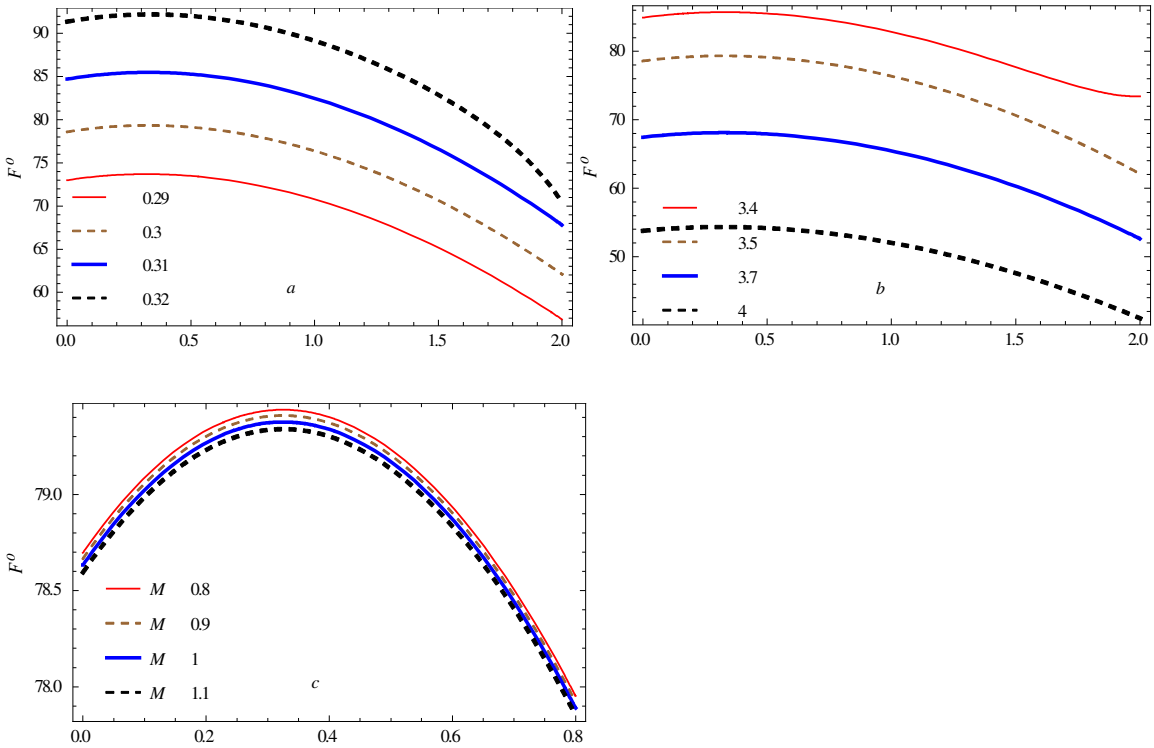

Fig.8 showing variation of $F^{(o)}$ vs. η, at $D_a=0.9, \lambda_1=0.1, q=0.5, \phi=0.1$, for (a) different values of ε, at $M=1.1, \alpha=3.5$, (b) different values of couple-stress parameter α, at $M=1.1, \varepsilon=0.3$, and (c) different values of magnetic parameter M, at $\alpha=3.5, \varepsilon=0.3$.

Fig.9 shows that the variation of $F^{(o)}$ vs. ϕ. We see that $F^{(o)}$ decreases with the increasing of ε, while $F^{(o)}$ increases with the increasing of any one of α or M.

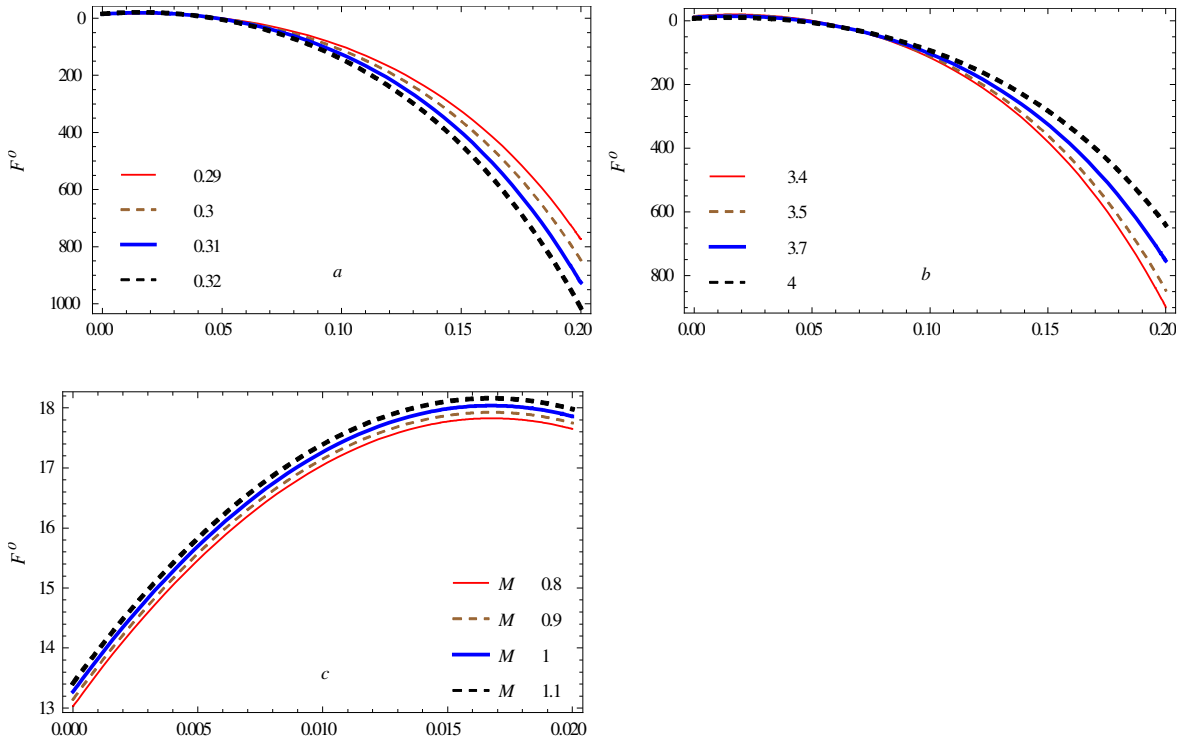

Fig.9 showing variation of $F^{(o)}$ vs. ϕ, at $D_a=0.9, \lambda_1=0.1, q=0.5, \eta=0.5$, for (a) different values of ε, at $M=1.1, \alpha=3.5$, (b) different values of couple-stress parameter α, at $M=1.1, \varepsilon=0.3$, and (c) different values of magnetic parameter M, at $\alpha=3.5, \varepsilon=0.3$.

Fig.10 shows that the variation of $F^{(o)}$ vs. q. In (a) we see that $F^{(o)}$ decreases with the increasing of ε in $q<0.62$, and $F^{(o)}$ increases with the increasing of ε when $q>0.62$. From (b) it is found that $F^{(o)}$ increases with the increasing of α in $q<0.719$, and $F^{(o)}$ decreases with the increasing of α when $q>0.719$. And (c) show that $F^{(o)}$ increases with the increasing of M.

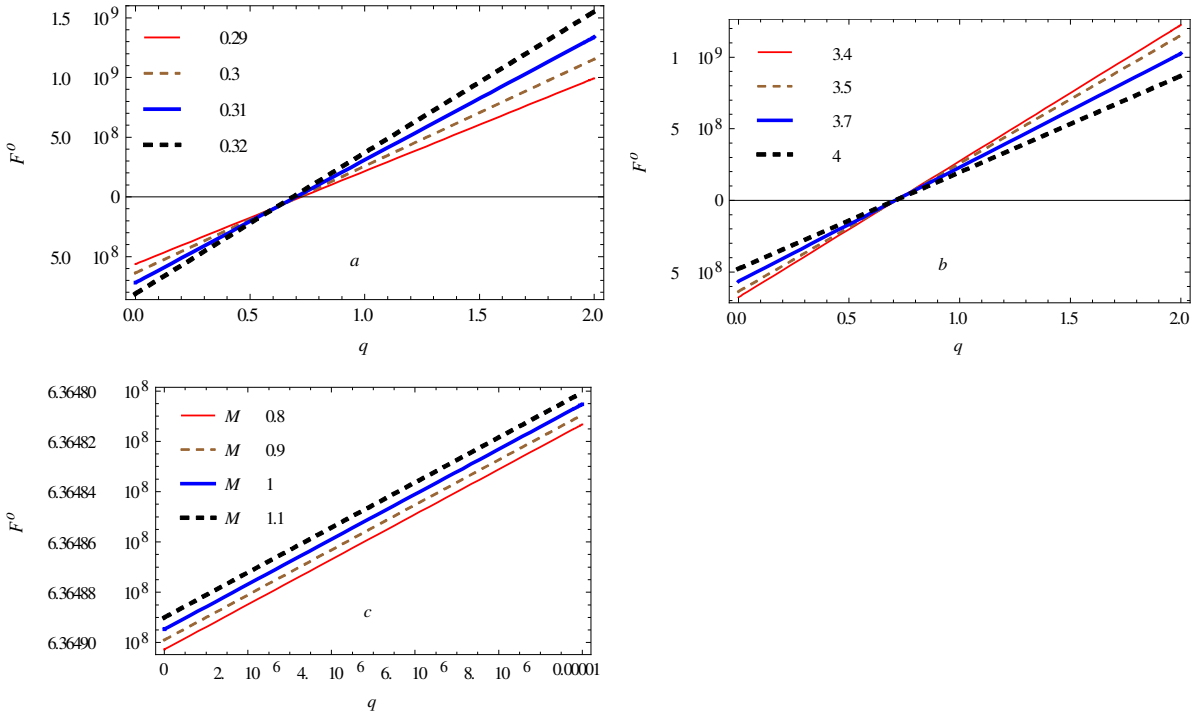

Fig.12 showing variation of $F^{(o)}$ vs. q, at D_a=0.9,λ_1=0.1,ϕ=0.5,η=0.5, for (a) different values of ε, at $M=1.1,\alpha=3.5$, (b) different values of couple-stress parameter α, at $M=1.1,\varepsilon=0.3$, and (c) different values of magnetic parameter M, at $\alpha=3.5,\varepsilon=0.3$.

Fig.11 shows that effects of the parameters P_r, R_n, and R_e on the temperature distribution function θ is direct, means θ increases with the increasing of any one of these parameters with fixed others when $0<r<3$, and then oscillatory. Also $\theta>0$ when $r<1.1754$, and $\theta<0$ when $r>1.1754$.

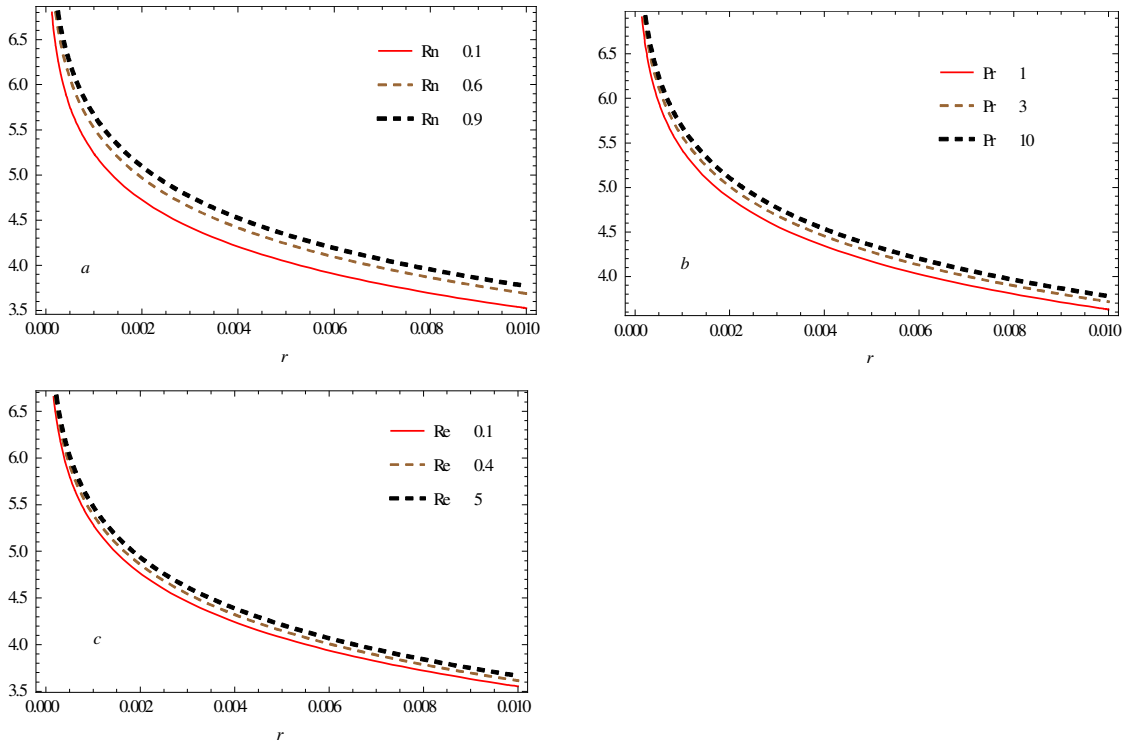

Fig.11 showing variation of temperature θ vs. r, at Ω=1,r_1=0.3,z=0.1,ϕ=0.3, for (a) different values of R_n, at $P_r = 2, R_e = 2$, (b) different values of P_r, at $R_n = 2, R_e = 0.8$, and (c) different values of R_e, at $P_r = 2, R_n = 0.1$.

7. Trapping phenomona

The formation of an internally circulating bolus of fluid by closed streamlines is called trapping and this trapped bolus is pushed ahead along with the peristaltic wave. The effects of M, α, D_a, λ_1, ε, ϕ, q, and η on trapping can be seen through Figs.12-19. Fig.12 show that the size of the trapped bolus decrease with the increase in M, also at M =0.34 a new region of trapped bolus appears near the flat wall of canal and increase in size with the increase in M. Fig.13 is plotted, the effect of α on trapping, the size of the trapped bolus decrease with the increase in α, also at α =3.7 the trapped bolus disappear to wave near the upper wall of canal. Fig.14 show that the size of the trapped bolus increase with the increase in D_a, and at D_a =1.2 the trapped bolus disappear to wave near the upper wall. Fig.15, show that the size of the trapped bolus increase with the increase in λ_1. Fig.16, depicts the variation of ε on the trapping phenomena. The size of the trapped bolus increase with the increase in ε near the upper wall, while at ε =0.2469 a new region of trapped bolus appears near the flat wall of canal and disappear at ε =0.3815.

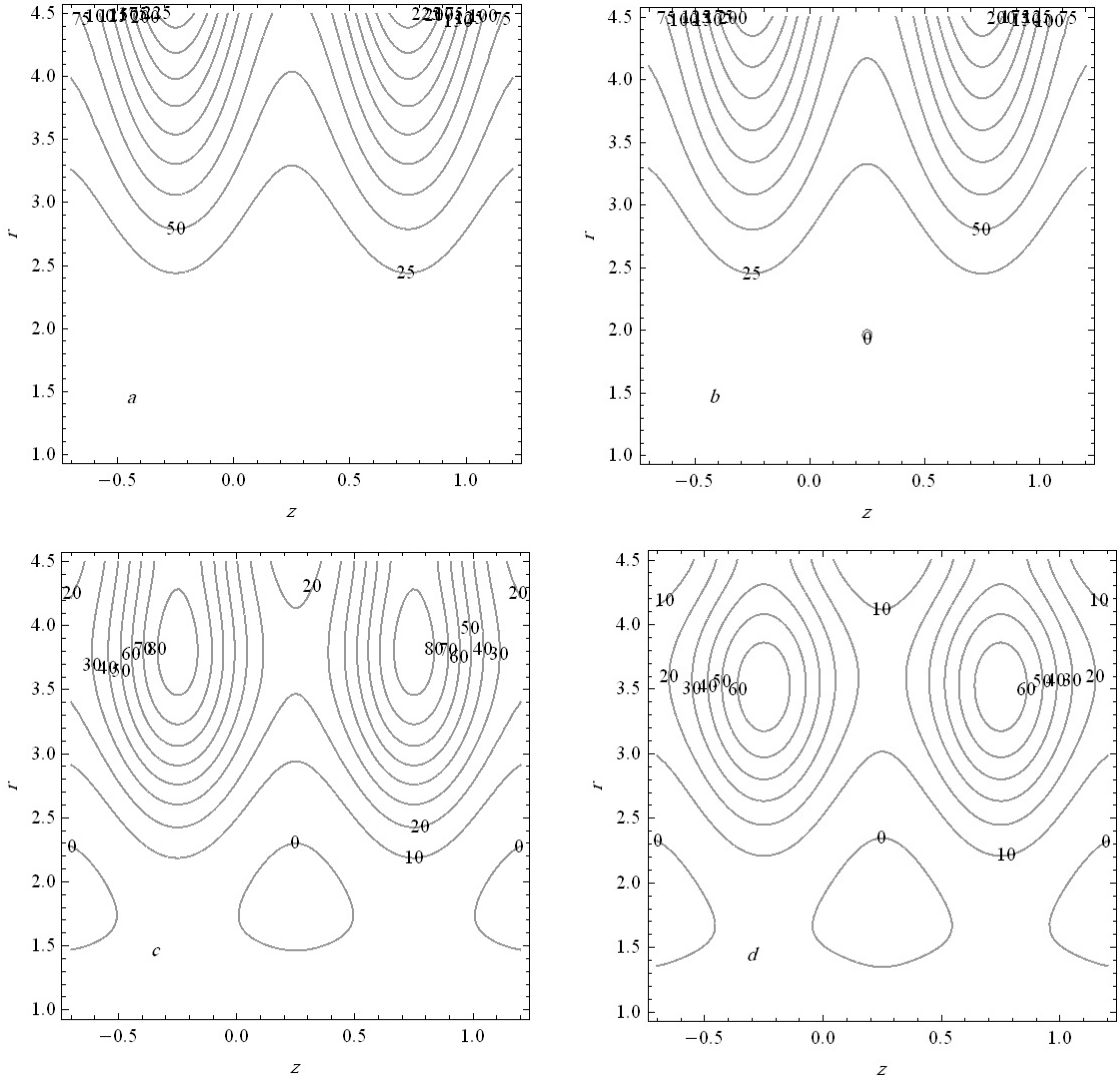

Fig.12 Graph of the streamlines for four different values of magnetic parameter M ; (a) $M = 0$, (b) $M = 0.34$, (c) $M = 1$, and (d) $M = 1.19$ at $D_a = 0.9, \lambda_1 = 0.1, \phi = 0.1, \alpha = 3.5, \varepsilon = 0.3, \eta = 0.5, q = 0.5$.

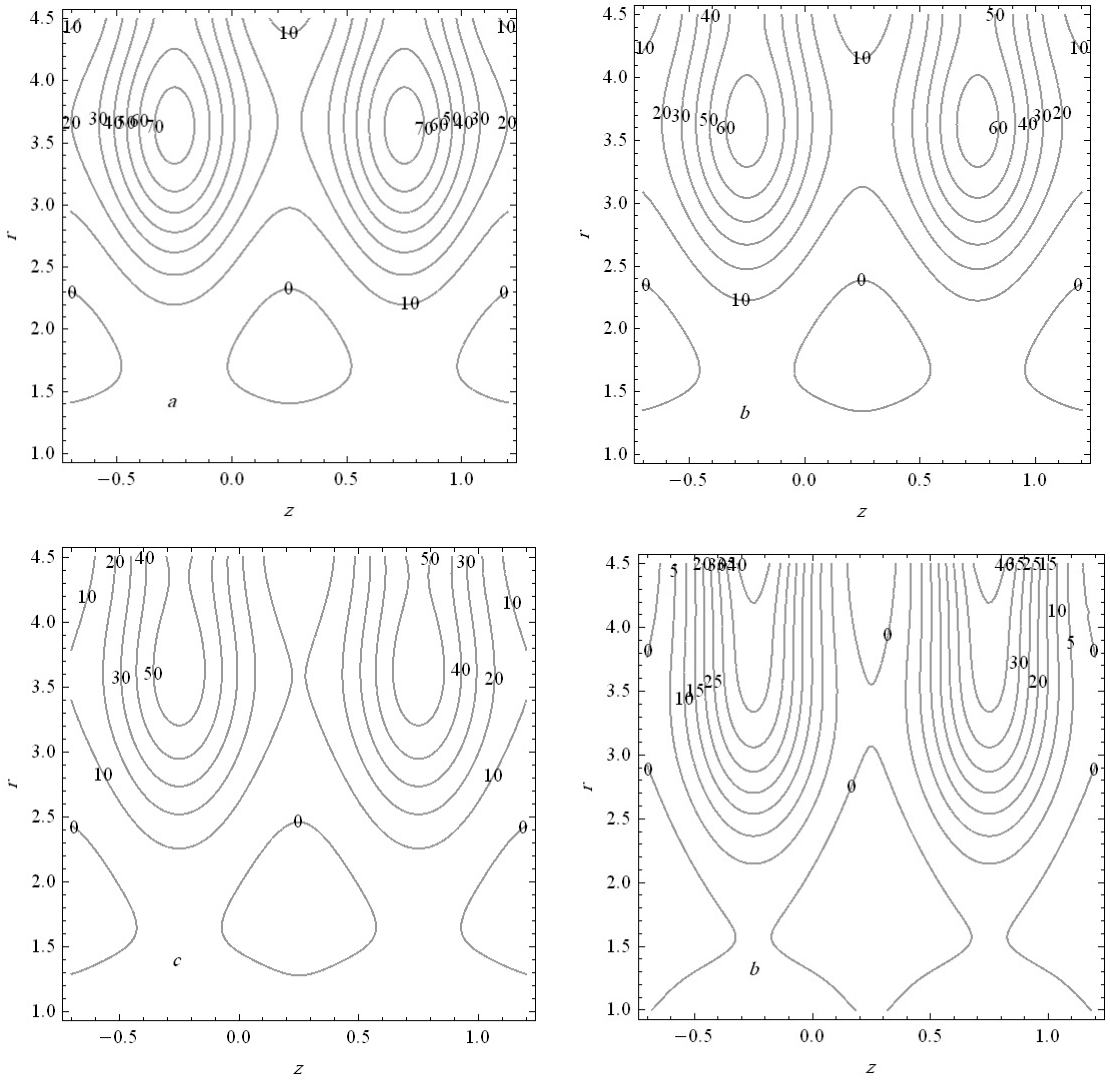

Fig.13 Graph of the streamlines for four different values of couple-stress parameter α ; (a) α = 3.5, (b) α = 3.6, (c) α = 3.7, and (d) α = 4 at $M=1.1, D_a=0.9, \lambda_1=0.1, \phi=0.1, \varepsilon=0.3, \eta=0.5, q=0.5$.

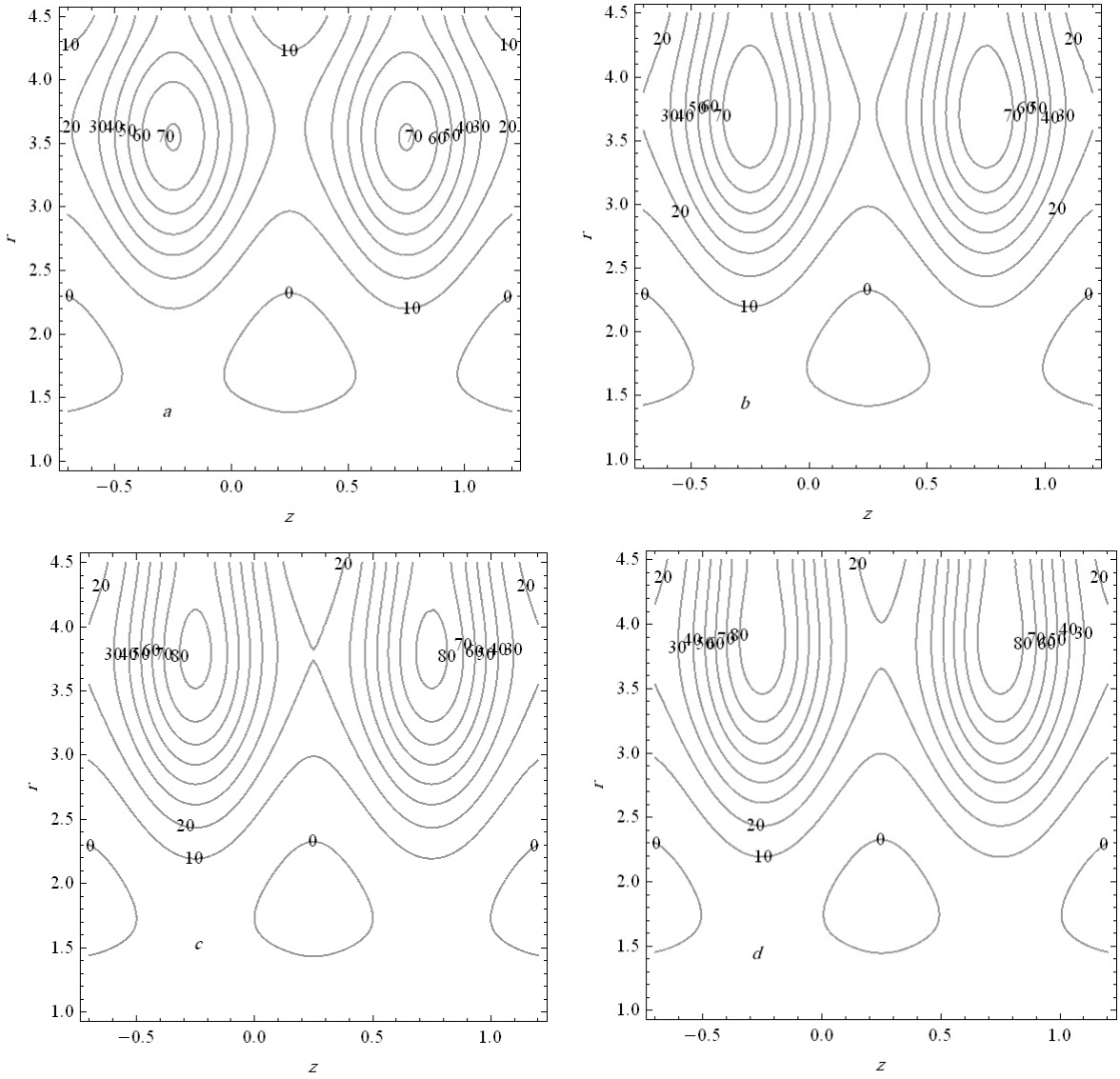

Fig.14 Graph of the streamlines for four different values of Darcy number D_a; (a) D_a = 0.8, (b) D_a = 1, (c) D_a = 1.1, and (d) D_a = 1.2 at $M=1.1, \lambda_1=0.1, \phi=0.1, \alpha=3.5, \varepsilon=0.3, \eta=0.5, q=0.5$.

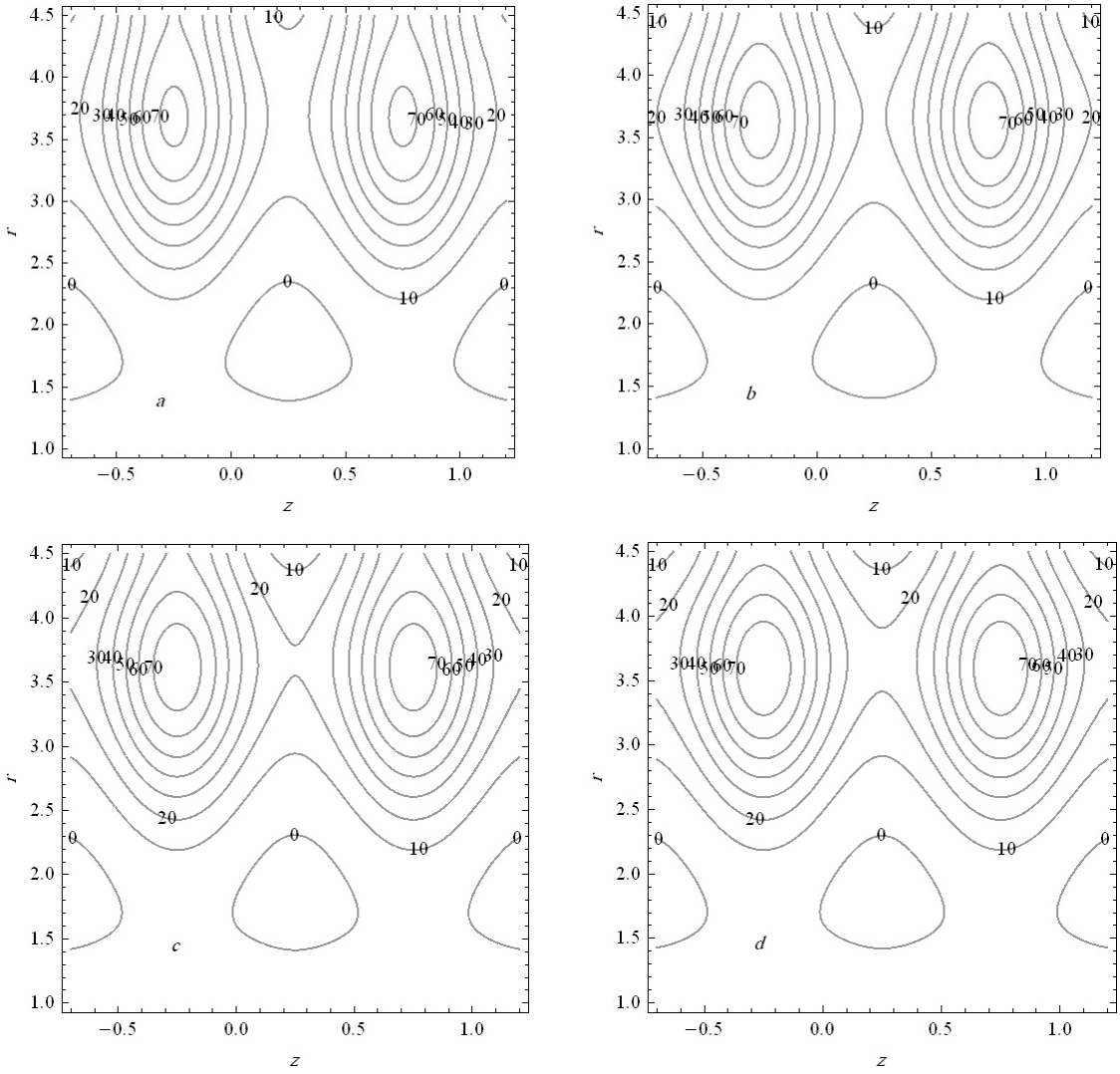

Fig.15 Graph of the streamlines for four different values of λ_1; (a) $\lambda_1 = 0.07$, (b) $\lambda_1 = 0.1$, (c) $\lambda_1 = 0.13$, and (d) $\lambda_1 = 0.14$ at $M=1.1, D_a=0.9, \phi=0.1, \alpha=3.5, \varepsilon=0.3, \eta=0.5, q=0.5$.

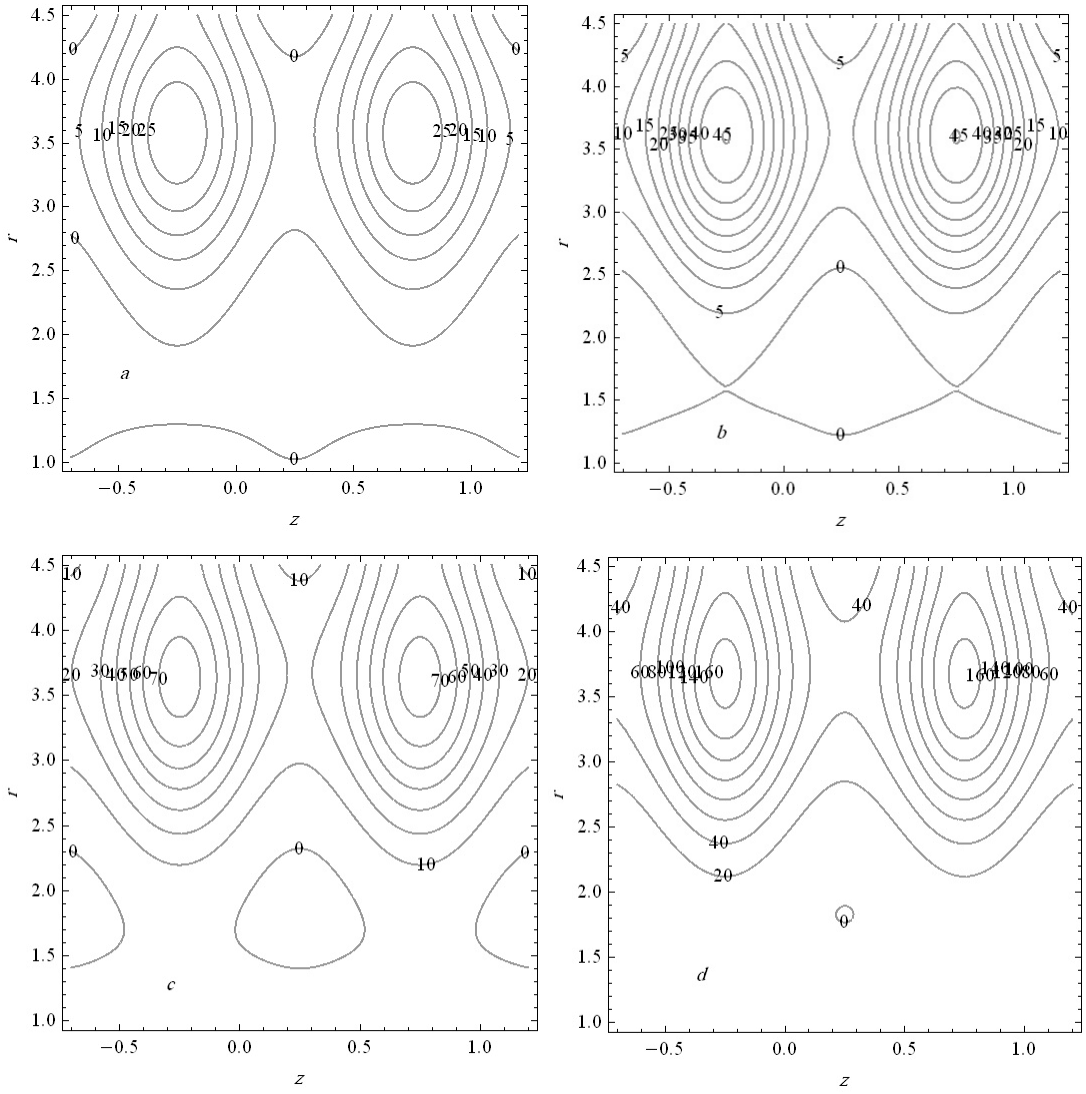

Fig.16 Graph of the streamlines for four different values of ε; (a) $\varepsilon = 0.2$, (b) $\varepsilon = 0.2467$, (c) $\varepsilon = 0.3$, and (d) $\varepsilon = 0.38$ at $M=1.1, D_a=0.9, \phi=0.1, \alpha=3.5, \lambda_1=0.1, \eta=0.5, q=0.5$.

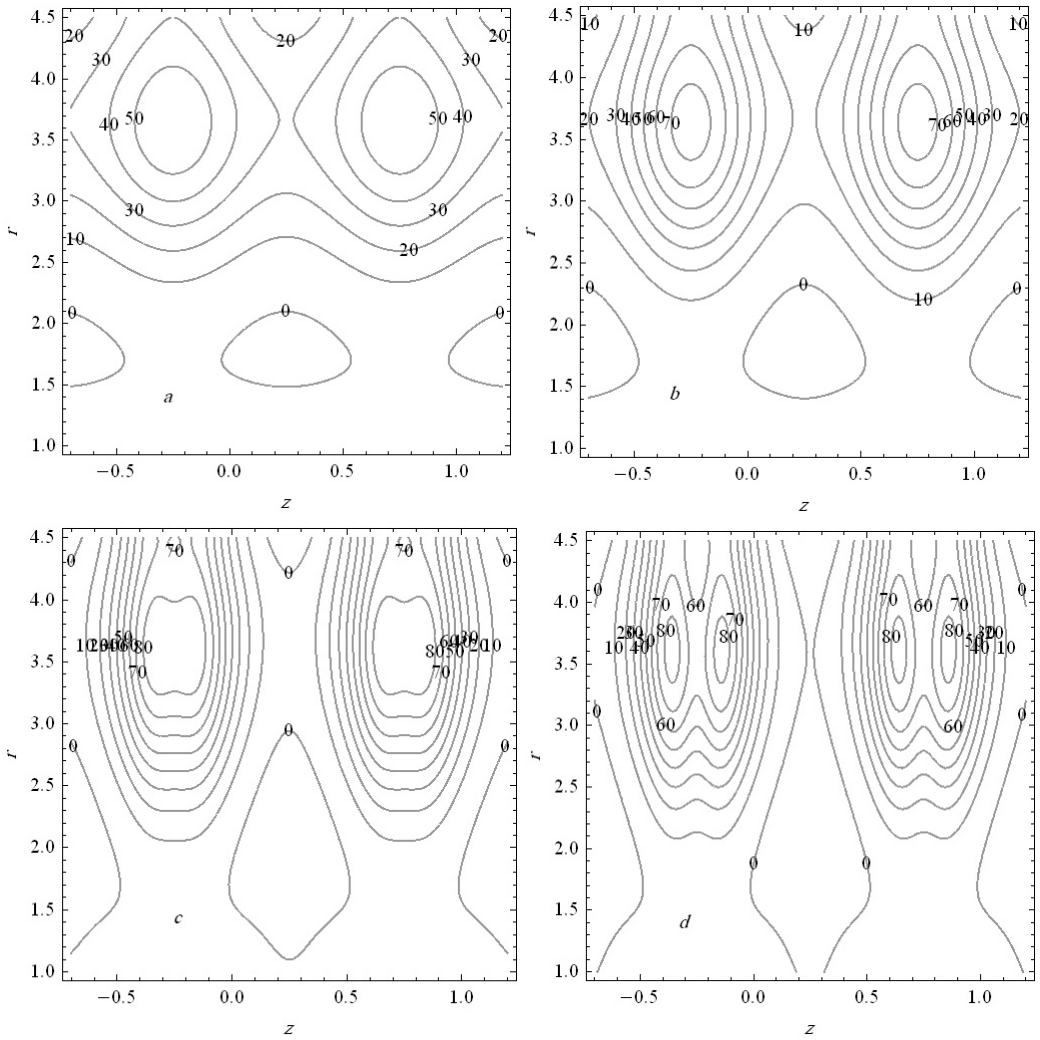

Fig.17 Graph of the streamlines for four different values of ϕ; (a) $\phi = 0.05$, (b) $\phi = 0.1$, (c) $\phi = 0.2$, and (d) $\phi = 0.23$ at $M = 1.1, D_a = 0.9, \varepsilon = 0.3, \alpha = 3.5, \lambda_1 = 0.1, \eta = 0.5, q = 0.5$.

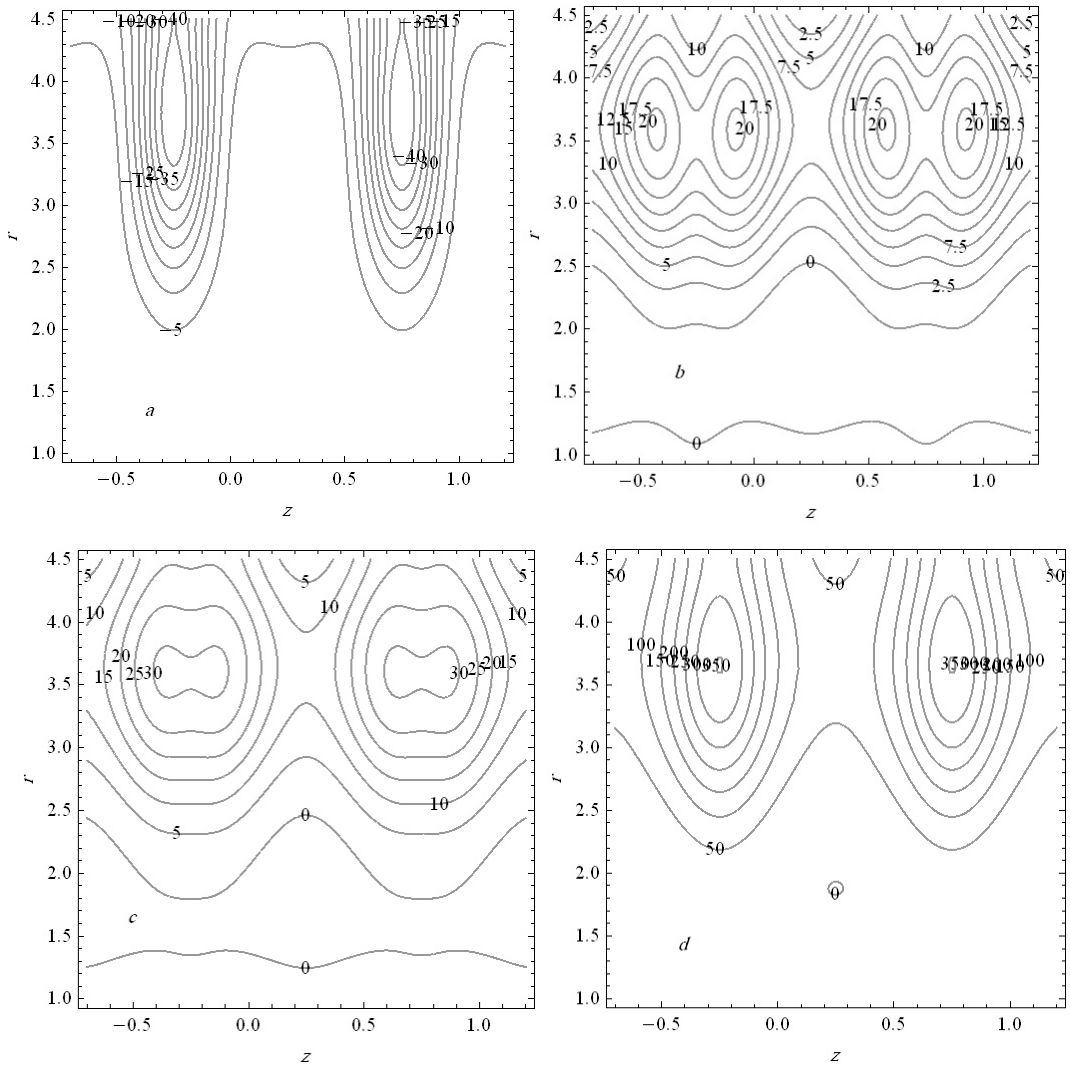

Fig.18 Graph of the streamlines for four different values of q; (a) $q = 0.1$, (b) $q = 0.3$, (c) $q = 0.5$, and (d) $q = 1.4$ at $M=1.1, D_a=0.9, \varepsilon=0.3, \alpha=3.5, \lambda_1=0.1, \eta=0.5, \phi=0.1$.

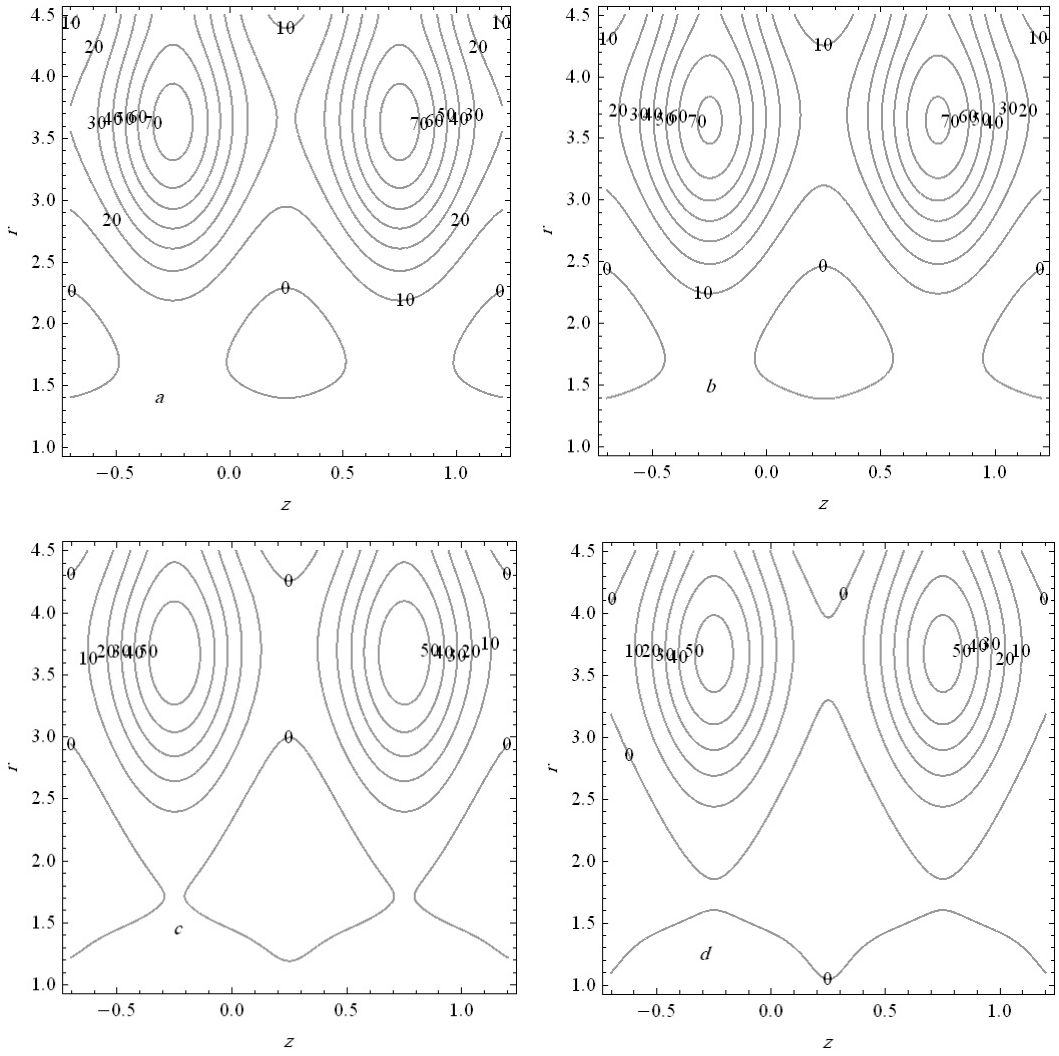

Fig.19 Graph of the streamlines for four different values of η; (a) η=0.3, (b) η=1, (c) η=1.65, and (d) η=1.9 at M=1.1, D_a=0.9, ε=0.3, α=3.5, λ_1=0.1, q=0.5, ϕ=0.1.

8- Concluding remarks

We have presented a theoretical approach to study the annulus peristaltic flow of a couple stress with heat and mass transfer of a Jeffery fluid in a tube through porous medium. The present analysis can serve as model which may help in understanding the mechanism of physiological flows in an annulus for fluids behaving like a couple stress fluid. From the point of view of mechanics, it is interesting to note how the peristaltic motion is influenced by the applied pressure gradient. Here we have analyzed the peristaltic flow through a gap between two coaxial tubes, the inner tube is rigid and the outer one has wave trains moving independently, the gap between them is filled with an incompressible viscous couple stress fluid (as a blood model). A long wavelength approximation is adopted. The exact expressions for axial velocity of the fluid, stream function and the axial pressure gradient are obtained analytically. Numerical integrations are used to analyze the novel features of pumping and trapping. The main findings can be summarized as follows:

1- The variation of pressure rise Δp as a function of the couple stress fluid parameter q for various values of other physical parameters indicate that in the pumping region $\Delta p > 0$, an increase of α decreases the pumping rate Δp , and the copumping region $\Delta p < 0$, the pumping rate increases by increasing α. There is a linear relation between q and Δp.

2- The variation of pressure rise Δp as a function of η for various values of other physical parameters indicate that in the pumping region $\Delta p > 0$, an increase of α decreases the pumping rate Δp, and the copumping region $\Delta p < 0$, the pumping rate increases by increasing α. The effect of parameter ε on Δp is opposite to the effect of α on Δp vs. η. The relation between η and Δp is a nonlinear.

3- The variation of pressure rise Δp as a function of ϕ for various values of other physical parameters indicate that in the pumping region $\Delta p > 0$ an increase of α decreases the pumping rate Δp, and the copumping region $\Delta p < 0$, the pumping rate increases by increasing α. There is a nonlinear relation between ϕ and Δp.

4- The variation of the outer and inner friction forces $F^{(o)}$ and $F^{(i)}$ appear at the outer and inner surfaces of the tubes, respectively, as a function of q, η, and ϕ, respectively, for various values of other physical parameters indicate that the outer friction $F^{(o)}$ has a greater value (positive or negative) than the inner friction $F^{(i)}$. The effects of $D_a, \lambda_1, M, \varepsilon$, and α on any of $F^{(o)}$ and $F^{(i)}$ can be considered to have similar effects of these parameters on of pressure rise Δp but with a reflection about the horizontal axis. There is a nonlinear relation between η, and ϕ vs. the friction forces.

References

[1] T. Hayat, A. H. Kara, E. Momoniat, Exact flow of a third grade fluid on a porous wall, Internat, J. Non-Linear Mech. 38(2003) 1533.
[2] T. Hayat, A. H. Kara, Couette flow of a third grade fluid with variable magnetic field, Math. Comput. Modelling 43 (2006) 132.
[3] T. Hayat, S. B. Khan, M. Khan, The influence of Hall current on the rotating oscillating flows of an Oldroyd-B fluid in a porous medium, Non-Linear Dynam, 47 (4) (2007).
[4] C. Fetecau, C. Fetecau, On some axaial Couette flows of non-Newtonian fluids, Z. Angew. Math. Phys. 56 (2005) 1098.
[5] Wang-Long Li, An average flow model for couple stress fluids, Tribology Lett. 15 (2003) 279.
[6] V. K. Stokes, Couple stress fluid, Phys. Fluids 9 (1966) 1709.
[7] K. C. Valanis, C. T. Sun, Poiseuille flow of a fluid with couple stress with application to blood flow, Biorheology 6 (1969) 85.
[8] Hayat, T., Ahmad, N., Ali, N.: Effects of an endoscope and magnetic field on the peristalsis involving Jeffery fluid. Commun. Nonlinear Sci. Numer. Simul. 13, p.1581-1591 (2008)
[9] Hayat, T., Javed, M., Ali, N.: MHD Peristaltic transfer of a Jeffery fluid in a channel with compliant walls and porous space. Transp. Porous Media 74, p.259-274 (2008)
[10] Srinivas, S., Kothandapani, M.: The influence of heat and mass transfer on MHD peristaltic flow through a porous space with compliant walls, Appl. Math. Comput. 213, p.197-208 (2009)
[11] Nadeem S. and Akbar N. S., Effect of temperature dependent viscosity on peristaltic flow of a Jeffery-six constant fluid in a non-uniform vertical tube, Comm. In Nonlinear Science and Numerical Simulation.

[12] Kothandapani M. and Srinivas, S., Peristaltic transport in an asymmetric channel with heat transfer, Int. Comm. In Heat and Mass Transfer, 35, p.514-522 (2008).
[13] Kothandapani M. and Srinivas, S., On the influence of wall properties in the MHD peristaltic transport with heat transfer and porous medium, App. Math. And Comp. 372, p.4586-4591 (2008).
[14] Hayat T. and Ali N., Peristaltic motion of a Jeffery fluid under the effect of a magnetic field in a tube, Comm. In Nonlinear Sci. and Numerical Simulation, 13, p.1343-1352 (2008).
[15] El-Dabe N. T. et. al., Rivlin –Ericksen fluid in tube of varying cross-section with mass and heat transfer, Z. Naturforsch., 57,p. 863-873 (2002).
[16] El-Dabe N. T. et. al., MHD peristaltic flow of non-Newtonian fluid through a porous medium in circular cylindrical tube, Bull. Cal. Math. Soc., 99, p.123-136 . (2007).
[17] El-Dabe N. T. et. al., Peristaltically induced transport of a MHD biviscosity fluid in a non-uniform tube, Physic A, 383, p.253-266 (2007).
[18] A. H. Shapiro, M. Y. Jaffrin, S. L. Weinberg, Peristaltic pumping with long wavelengths at low Reynolds number. J. Fluid Mech. 37, p. 799-825 (1969).

The IISTE is a pioneer in the Open-Access hosting service and academic event management. The aim of the firm is Accelerating Global Knowledge Sharing.

More information about the firm can be found on the homepage:
http://www.iiste.org

CALL FOR JOURNAL PAPERS

There are more than 30 peer-reviewed academic journals hosted under the hosting platform.

Prospective authors of journals can find the submission instruction on the following page: http://www.iiste.org/journals/ All the journals articles are available online to the readers all over the world without financial, legal, or technical barriers other than those inseparable from gaining access to the internet itself. Paper version of the journals is also available upon request of readers and authors.

MORE RESOURCES

Book publication information: http://www.iiste.org/book/

IISTE Knowledge Sharing Partners

EBSCO, Index Copernicus, Ulrich's Periodicals Directory, JournalTOCS, PKP Open Archives Harvester, Bielefeld Academic Search Engine, Elektronische Zeitschriftenbibliothek EZB, Open J-Gate, OCLC WorldCat, Universe Digtial Library , NewJour, Google Scholar